

Determining cysteine oxidation status using differential alkylation

Birgit Schilling^a, Chris B. Yoo^a, Christopher J. Collins^b, Bradford W. Gibson^{a,c,*}

^a The Buck Institute for Age Research, Novato, CA 94945, USA

^b Stanford Research Institute, 333 Ravenswood Ave., Menlo Park, CA 94025, USA

^c Department of Pharmaceutical Chemistry, The University of California, San Francisco, CA 94143-0446, USA

Received 11 June 2004; accepted 14 June 2004

Available online 20 July 2004

Abstract

Oxidative damage to proteins plays a major role in aging and in the pathology of many degenerative diseases. Under conditions of oxidative stress, reactive oxygen and nitrogen species can modify key redox sensitive amino acid side chains leading to altered biological activities or structures of the targeted proteins. This in turn can affect signaling or regulatory control pathways as well as protein turnover and degradation efficiency in the proteasome. Cysteine residues are particularly susceptible to oxidation, primarily through reversible modifications (e.g., thiolation and nitrosylation), although irreversible oxidation can lead to products that cannot be repaired in vivo such as sulfonic acid. This report describes a strategy to determine the overall level of reversible cysteine oxidation using a stable isotope differential alkylation approach in combination with mass spectrometric analysis. This method employs ¹³C-labeled alkylating reagents, such as *N*-ethyl-[1,4-¹³C₂]-maleimide, bromo-[1,2-¹³C₂]-acetic acid and their non-labeled counterparts to quantitatively assess the level of cysteine oxidation at specific sites in oxidized proteins. The differential alkylation protocol was evaluated using standard peptides and proteins, and then applied to monitor and determine the level of oxidative damage induced by diamide, a mild oxidant. The formation and mass spectrometric analysis of irreversible cysteine acid modification will also be discussed as several such modifications have been identified in subunits of the mitochondrial electron transport chain complexes. This strategy will hopefully contribute to our understanding of the role that cysteine oxidation plays in such chronic diseases such as Parkinson's disease, where studies in animal and cell models have shown oxidative damage to mitochondrial Complex I to be a specific and early target.

© 2004 Elsevier B.V. All rights reserved.

Keywords: Oxidative stress; Cysteine oxidation; Differential alkylation; Stable isotopes

1. Introduction

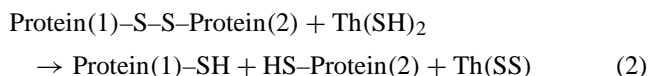
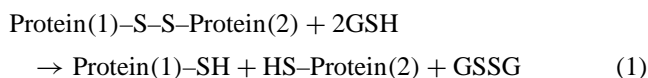
Oxidative stress is a major contributor to human diseases and aging [1]. A number of amino acids have been shown to undergo post-translational modifications under conditions of oxidative stress [2]. Lysine, arginine, proline and threonine residues, for example, can be oxidized to yield aldehydes and ketones, often referred to as 'carbonylation' products [3,4]. Deamidation of asparagine to isoaspartate and D-aspartate has also been reported in an age-related fashion [5,6]. Possibly more relevant to exerting a deleterious effect on biological activity is the modification of tyrosine, methionine and cysteine by reactive oxygen (ROS) and nitrogen species (RNS). Tyrosine, for example, is known to undergo

dimerization to *o,o'*-dityrosine or react with peroxynitrite (or other reactive nitrogen species) to form 3-nitrotyrosine [7–9]. Methionine residues can be easily oxidized to methionine sulfoxide under physiological conditions, although this modification can be repaired in vivo by methionine sulfoxide reductases [10,11].

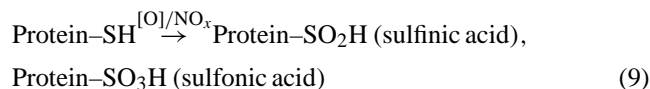
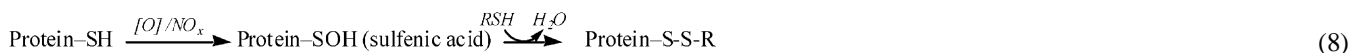
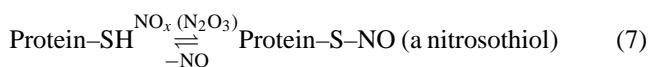
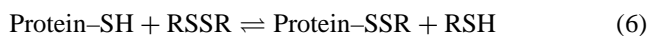
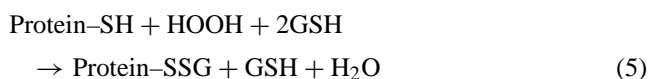
Cysteine residues, however, are perhaps the most sensitive to oxidation and can result in a wide range of modifications, including reaction with glutathione and peroxynitrite (for review, see [12]). Reactive oxygen species can affect changes in the redox status of susceptible cysteine residues and thus potentially alter a protein's activity, structure and/or ligand binding capacity. This reactivity has been suggested to provide key cysteine residues with unique roles as redox 'sensors' or 'switches', as cysteines have both catalytic and metal binding capacities that are dependent on its oxidative status [13]. Unlike most amino acid oxidation

* Corresponding author. Tel.: +1-415-209-2032; fax: +1-415-209-2231.
E-mail address: bgibson@buckinstitute.org (B.W. Gibson).

products discussed above (with the exception of methionine), many cysteine oxidative modifications can be reversed *in vivo* by the action of glutathione (GSH) or thioredoxin (Th(SH)₂) [1]. For example, protein disulfides can be repaired by exchange reactions with these disulfides to regenerate the reduced sulfhydryl protein products (Eqs. (1) and (2)). Similarly, many of the oxidative products involving cysteine can be reversed *in vitro* by treatment with mild reductants such as DTT. The accumulation of such oxidized products may contribute to an overall imbalance in the complex set of oxidants, reductants and repair mechanisms that orchestrate the redox state of a cell or neuron that may ultimately underlie the progression of many degenerative diseases:



The oxidation of cysteine residues in proteins can take several paths, giving rise to a number of different products. For example, cysteines can form intramolecular disulfides if two free cysteines are in close proximity (Eq. (3)). More likely, under conditions of oxidative stress, sulfhydryls would be expected to undergo reversible oxidations to form mixed disulfides with glutathione or GSSG (Eqs. (4) and (5)) or other types of sulfhydryl-containing species such as free cysteine, cysteamine or homocysteine (Eq. (6)). Cysteines can also be *S*-nitrosylated by reactive nitrogen species (e.g., NO_x = nitric oxide, peroxyxynitrite, N₂O₃ or others) or NO-carriers to form *S*-nitrosocysteine [14] (Eq. (7)) or sulfenic acid [15], the latter of which can react with other sulfhydryl-containing compounds (GSH or RSH) to form mixed disulfides (Eq. (8)). Lastly, cysteines can also be irreversibly oxidized to their corresponding sulfinic or sulfonic acids [16,17] (Eq. (9)):



Analytical methods to determine the type and sites of oxidative damage in proteins, particularly targeting cysteine oxidation, are generally lacking, although several recent protocols appear promising. In particular, the development and use of the mitochondrial-specific probes by Murphy and colleagues [18,19], i.e., iodobutyltriphenylphosphonium (IBTP) and thiobutyltriphenylphosphonium (TBTP), that target free sulfhydryl groups or oxidized sulfhydryls have opened new avenues to probe the redox states of cysteines under physiologically relevant conditions. IBTP reacts irreversibly with ‘free thiols’ (non-oxidized) to produce the corresponding protein-thioether while TBTP equilibrates with endogenous thiols to produce mixed disulfides and protein disulfide bonds under conditions of oxidative stress. In other approaches, proteins have been isolated from tissues or subjected to oxidative reagents and their resulting products have undergone analysis using mass spectrometry techniques. For example, for sarcoplasmic reticulum Ca-ATPase, a number of oxidation-sensitive amino acids or peptides were identified by HPLC-MS techniques after treatment with H₂O₂ [20] and peroxyxynitrite [21], including bityrosine, 3-nitrotyrosine, GSH-adducts of cysteine (*S*-glutathiolation), and *S*-nitrosylated cysteine, among others. Likewise, in mass spectrometry-based studies of α-A-crystallin [22], significant differences were found in the oxidation states of Cys-131 and Cys-142 as associated with disease (cataractous lenses and lens opacification).

Cysteine oxidation seems to play a major role in several neurodegenerative diseases. Nitric oxide (NO) has been proposed to be involved in acute CNS injury produced by cerebral ischemia. Gu et al. [23] reported NO formation and *S*-nitrosylation for matrix metalloproteinases observed during ischemia. Recently, Chung et al. described *S*-nitrosylation of parkin regulating ubiquitination and effecting parkin’s protective function [24]. We are particularly interested in investigating oxidative stress in Parkinson’s disease (PD) where a largely reversible loss of NADH-dehydrogenase (electron transport chain Complex I) activity is seen under conditions of glutathione depletion in dopaminergic rat cell lines that serve as disease model for PD [25]. The loss of Complex I activity is recoverable by treatment with DTT, and is most likely due to oxidative damage of cysteines such as *S*-glutathiolation and *S*-nitrosylation, adducts that can be easily reversed by treatment with DTT. The products of these reactions, mixed disulfides and *S*-nitrosocysteines, are therefore the most likely products leading to the reversible loss of protein activity due to oxidative stress. *S*-Nitrosocysteine, however, has been reported to decompose at high pH, elevated

temperature, and even by excessive exposure to light that may complicate analysis on a molecular level [26]. The 45–46 known protein subunits of human mitochondrial Complex I contain at least 133 cysteine residues and present a formidable analytical challenge to identify the site or sites that are responsible for the loss of activity. Therefore, in this report we describe our efforts to develop more appropriate analytical tools using cysteine alkylating reagents containing stable isotopes to investigate the redox status of cysteine modifications in complex protein samples, such as we will encounter in our ongoing studies of Complex I and other electron transport chain complexes.

2. Experimental

Standard peptide Arg⁸-Vasopressin (CYFQNCPRG-NH₂) was purchased from Bachem (Torrance, CA), major histocompatibility complex (MHC) antigen H-2K^b fragment 163–174 (TCVEWLRRLKLN), standard proteins aldolase (rabbit), β -lactoglobulin (bovine), and ovalbumin (chicken) were obtained from Sigma (St. Louis, MO). For proteolysis, sequencing grade, modified trypsin (porcine) was purchased from Promega (Madison, WI), sequencing grade chymotrypsin (bovine) and Glu-C (*Staphylococcus aureus*) were purchased from Roche (Indianapolis, IN). Additional reagents for protein chemistry including bromoacetic acid, iodoacetic acid, *N*-ethyl-maleimide (NEM), and dithiothreitol (DTT), and diamide (1,1'-azobis(*N,N*-dimethylformamide)) were obtained from Sigma (St. Louis, MO). Stable isotope containing reagents, such as [1,4-¹³C₂]-maleic anhydride, [1,2-¹³C₂]-bromoacetic acid, and [2-¹³C]-iodoacetic acid were obtained from Cambridge Isotopes (Andover, MA). HPLC solvents such as acetonitrile and water were obtained from Burdick & Jackson (Muskegon, MI). For MALDI-MS experiments a matrix solution of α -cyano-4-hydroxycinnamic acid in acetonitrile/methanol was purchased from Agilent Technologies (Palo Alto, CA).

2.1. Synthesis of *N*-ethyl-[1,4-¹³C₂]-maleimide (Compound 3)

A dry pressure flask was charged with [1,4-¹³C₂]-maleic anhydride **1** as seen in Scheme 2 (100 mg, 1.01 mmol) and 5 mL of 2 M ethylamine in tetrahydrofuran (THF). The reaction vessel was sealed and stirred at 65 °C for 2 h. Then, the reaction mixture was cooled to 25 °C under argon (Ar) and solvent was removed under vacuum (30 °C, 8 Torr) to give 140 mg (96%) of the acid amide intermediate **2** as an off-white solid. Compound **2** was taken up in 3 mL acetic anhydride and warmed to 65 °C for 2 h. The reaction mixture was cooled to 25 °C under Ar, and the solvent was removed under vacuum. The resulting viscous residue was stirred at 25 °C with saturated aqueous potassium carbonate for 0.5 h. The aqueous layer was extracted with 4 × 10 mL

portions of ethyl acetate, dried over magnesium sulfate, filtered and dried under vacuum (30 °C, 8 Torr) to give 110 mg (90%) of the crude *N*-ethyl-[1,4-¹³C₂]-maleimide **3** as an off-white solid. The crude product **3** was then further purified via HPLC.

2.2. Differential cysteine alkylation using two alkylating reagents and proteolytic digestion of proteins (in solution)

Alkylating reagents such as bromoacetic acid, iodoacetic acid, NEM, and the stable isotope versions thereof were used. For the stepwise alkylation method using stable isotope reagents, the following experimental procedures were performed (in all cases reagent excess refers to molar excess over number of Cys residues per protein). Typically, 50 μ g of protein were diluted with 50 mM NH₄HCO₃ buffer (pH 8.0) to yield protein concentrations of 10 μ M. Initially, proteins were alkylated with a 200-fold excess of alkylating reagent 1 (R₁X) at 37 °C, 60 min (in some cases a mild denaturant was added to make protein sulfhydryl groups more accessible, e.g., 2 M guanidine hydrochloride or acetonitrile). Subsequently, the reaction mixture was incubated with a 400-fold excess of L-cysteine to quench the alkylating reagent 1. Proteins were then fully denatured (40% acetonitrile) and reduced with a 1000-fold molar excess of DTT at 56 °C for 60 min, and then incubated with 3100-fold excess of alkylating reagent 2 (R₂X, 37 °C, 60 min). Aliquots of 10 μ g protein were diluted to final acetonitrile concentrations of 5–10%, and subsequently digested at 37 °C (or at room temperature) overnight using the following proteolytic enzymes in individual experiments, 200 ng trypsin, 200 ng chymotrypsin, and 200 ng Glu-C, respectively. The proteolytic digestion mixtures were desalted using C-18 ZipTips (Millipore, Billerica, MA), and subsequently analyzed by MALDI mass spectrometry and LC-ESI-MS/MS. Similar alkylation experiments were performed for the standard peptides; in those cases no digestion steps were added.

2.3. Mild protein oxidation using diamide and subsequent differential cysteine alkylation

Typically, 50 μ g of protein were diluted with 50 mM NH₄HCO₃ buffer (pH 8.0) to yield protein concentrations of 10 μ M. Proteins were subjected to oxidative stress by incubation with the mild oxidizing reagent diamide at room temperature using concentrations of 1, 10, 50, and 100 μ M diamide, respectively. Reaction mixtures were quenched after 15, 30, 60, and 120 min by addition of the first alkylating reagent 1 and incubation with R₁X at 37 °C, 120 min (in the presence of mild denaturant). As described in detail above for the differential alkylation protocol, subsequently the reaction mixtures were incubated with L-cysteine, denatured with acetonitrile and reduced with DTT (56 °C, 60 min), incubated with alkylating reagent 2 (R₂X, 37 °C, 60 min), then proteolyzed, and subjected to mass spectrometric analysis.

2.4. MALDI-TOF mass spectrometry

Mass spectra of digested gel spots were obtained by matrix-assisted laser desorption ionization time-of-flight (MALDI-TOF) mass spectrometry on a Voyager DE-STR plus (Applied Biosystems, Framingham, MA). All mass spectra were acquired in positive-ionization mode with reflectron optics. The instrument was equipped with a 337 nm nitrogen laser and operated under delayed extraction conditions; delay time 190 ns, grid voltage 66–70% of full acceleration voltage (20–25 kV). All peptide samples were prepared using a matrix solution consisting of 33 mM α -cyano-4-hydroxycinnamic acid in acetonitrile/methanol (1/1 v/v); 1 μ L of analyte (0.1–1 pmol of material) was mixed with 1 μ L of matrix solution, and then air-dried at room temperature on a stainless steel target. Typically, 50–100 laser shots were used to record each spectrum. The obtained mass spectra were externally calibrated with an equimolar mixture of angiotensin I, ACTH 1–17, ACTH 18–39, and ACTH 7–38.

2.5. Nano-HPLC-ESI-MS, MS/MS

In all cases, the proteolytic peptide mixtures were analyzed by reverse-phase nano-HPLC-ESI-MS, MS/MS (electrospray ionization, ESI). Briefly, peptides were separated on an Ultimate nanocapillary HPLC system equipped with a PepMapTM C18 nano-column (75 μ m I.D. \times 15 cm) (Dionex, Sunnyvale, CA) and CapTrap Micro-guard column (0.5 μ l bed volume, Michrom, Auburn, CA). Peptide mixtures were loaded onto the guard column and washed with the loading solvent (H₂O/0.05% formic acid, flow rate: 20 μ l/min) for 5 min, then transferred onto the analytical C18-nanocapillary HPLC column and eluted at a flow rate of 300 nL/min using the following gradient: 2% B (from 0 to 5 min), and 2–70% B (from 5 to 55 min). Solvent A consisted of 0.05% formic acid in 98% H₂O/2% ACN and solvent B consisted of 0.05% formic acid in 98% ACN/2% H₂O. The column eluant was directly coupled to a 'QSTAR Pulsar i' quadrupole orthogonal TOF mass spectrometer (MDS Sciex, Concord, Canada) equipped with a Protana nanospray ion source (ProXeon Biosystems, Odense, Denmark). The nanospray needle voltage was typically 2300 V in the HPLC-MS mode. Mass spectra (ESI-MS) and tandem mass spectra (ESI-MS/MS) were recorded in positive-ion mode with a resolution of 12 000–15 000 FWHM. For collision induced dissociation tandem mass spectrometry, the mass window for precursor ion selection of the quadrupole mass analyzer was set to ± 1 m/z . The precursor ions were fragmented in a collision cell using nitrogen as the collision gas. Spectra were calibrated in static nanospray mode using MS/MS fragment ions of a renin peptide standard (His immonium-ion with m/z at 110.0713, and b₈-ion with m/z at 1028.5312) providing a mass accuracy of ≤ 50 ppm.

2.6. Database searches for protein identification

Mass spectrometric data were analyzed with the in-house licensed bioinformatics database system RADARS (Genomic Solutions, Ann Arbor, MI) and Mascot (Matrix Sciences, London, United Kingdom). Routinely, MALDI-MS data were analyzed with RADARS using the search engine ProFound for Peptide Mass Fingerprints (PMF) matching against peptides from known protein sequences entered in publicly available protein databases (e.g. NCBI) using the following parameters: internal calibration using trypsin autolysis masses (m/z 842.5100 and 2211.1046), 100 ppm mass accuracy, two missed proteolytic cleavages allowed. In all cases, tryptic and chymotryptic digestion extracts of proteins were analyzed by HPLC-ESI-MS and MS/MS, these data were then submitted to the search engine Mascot that analyzes peptide sequence information from tandem mass spectra. Both search engines applied, provide a statistical scoring parameter, for example, ProFound searching PMF data uses the so-called 'expectation value', for data quality control [27]. The search engine Mascot uses a probability based 'Mowse Score' to evaluate data obtained from tandem mass spectra, e.g. for a score >37 , protein matches are considered significant [28].

2.7. Simulation of theoretical isotope patterns containing stable isotopes

The isotope pattern calculation program "Isotope v.1.6" was used for simulating isotope patterns to determine the ¹³C/¹²C ratio within cysteine modifications (determination of R₁X/R₂X ratio to subsequently determine the level of cysteine oxidation) written by Les Arnold (University of Waikato, New Zealand).

3. Oxidative modification and differential alkylation strategies

In living organisms and cells oxidative stress can cause severe protein damage, as well as lipid peroxidation and DNA damage. Fig. 1 shows a diagram displaying key reactive oxygen species and their precursors that can form upon oxidative stress. Sources for oxidative stress can be either endogenous (e.g. mitochondrial matrix, membrane oxidases, catechols and quinones, inflammatory products, and hypoxia-reperfusion/NOS) or exogenous (e.g. oxidants, such as diamide and H₂O₂, or xenobiotic quinones) [2]. Under oxidative stress, ROS such as superoxide anions (O₂^{•-}), superoxide radicals (HO₂[•]), hydroxyl radicals (OH[•]), and peroxynitrite (⁻ONO₂), can accumulate (see Fig. 1). Protective mechanisms exist, such as enzymatic antioxidant defense through the enzymes superoxide dismutase (SOD)/catalase peroxidase, and thioredoxin. Some non-enzymatic antioxidants, such as glutathione, Vitamins (C, E and K), and cofactors (NAD⁺/NADH, CoQ10) also contribute to "free radical

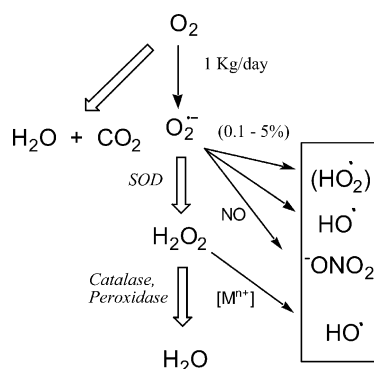


Fig. 1. Typically, oxygen is metabolized and converted into H_2O and CO_2 . Under oxidative stress, however, the production of reactive oxygen species (ROS) can be increased. The formation of superoxide anions ($\text{O}_2^{\bullet-}$) further leads to the generation of superoxide radicals (HO_2^\bullet), hydroxyl radicals (OH^\bullet), and in combination with nitric oxide (NO) to peroxynitrite ($^-\text{ONO}_2$). Metal $[\text{M}^{n+}]$ catalyzed reactions such as the Fenton–Weiss reactions can also contribute to hydroxyl radicals (OH^\bullet) formation. Enzymatic antioxidant defense is provided through the enzymes superoxide dismutase (SOD), catalase, and peroxidase.

quenching”. However, increased generation of ROS under conditions of prolonged oxidative stress can lead to severe protein oxidative damage, impact on signaling pathways, accumulation of damaged proteins, impairment of cellular function, senescence, and ultimately cell death. Such oxidative damage is presumed to play a major role in aging and age-related diseases.

As discussed previously, cysteine residues are most sensitive to oxidative stress. We have developed an efficient differential alkylation strategy using stable isotopes to determine redox states of cysteine residues within a protein, and to differentiate cysteines that exist in their reduced form (free sulfhydryls) from cysteines that exist in oxidized forms

(in disulfide bridges or as *S*-nitrosocysteine). Fig. 2 summarizes this strategy. In the top panel, a series of reversible oxidative products are shown for a reduced cysteine residue (sulfhydryl form), including the formation of glutathione adducts, intramolecular disulfide bridges (within one protein molecule), intermolecular disulfide bridges (within two protein molecules, dimer formation), and *S*-nitrosylation. Under prolonged oxidative stress, it is also possible that irreversible oxidation products can form, such as sulfonic acid. In the bottom panel for Fig. 2 (Panel B), a strategy is shown that describes a means to differentially label the free and oxidized cysteines through alkylation; proteins are first reacted with an alkylating reagent (alkylation reagent 1 or R_1X) to target all ‘freely accessible’ sulfhydryl groups (non-oxidized). Then after vigorous denaturation and reduction, proteins are incubated with a second alkylating reagent (R_2X), an analogous stable isotope reagent of R_1X , to label all remaining unreactive (oxidized) cysteines. (It should be noted that in the example given in Fig. 2, the irreversible sulfonic acid product would not be reduced under these condition and would remain unmodified.) After proteolysis and HPLC–MS analysis, one can then assign the relative amounts of the reduced versus (reversibly) oxidized cysteine by comparing the ion abundances of the peptide pairs now containing alkylating groups in their stable isotope and/or normal form, reflecting the redox state of the specific cysteine residue.

Scheme 1 shows alkylating reagents that we are currently employing for this differential alkylation strategy. Cysteine alkylating reagents that we have available in their normal and stable isotope version are the following, reagents for carboxymethylation: iodo- and/or bromoacetic acid ($2 \times ^{12}\text{C}$), [$2\text{-}^{13}\text{C}$]-iodoacetic acid ($1 \times ^{13}\text{C}$), and [$1,2\text{-}^{13}\text{C}_2$]-bromoacetic acid ($2 \times ^{13}\text{C}$); maleimide reagents: regular NEM ($2 \times ^{12}\text{C}$), and [$1,4\text{-}^{13}\text{C}_2$]-NEM ($2 \times ^{13}\text{C}$);

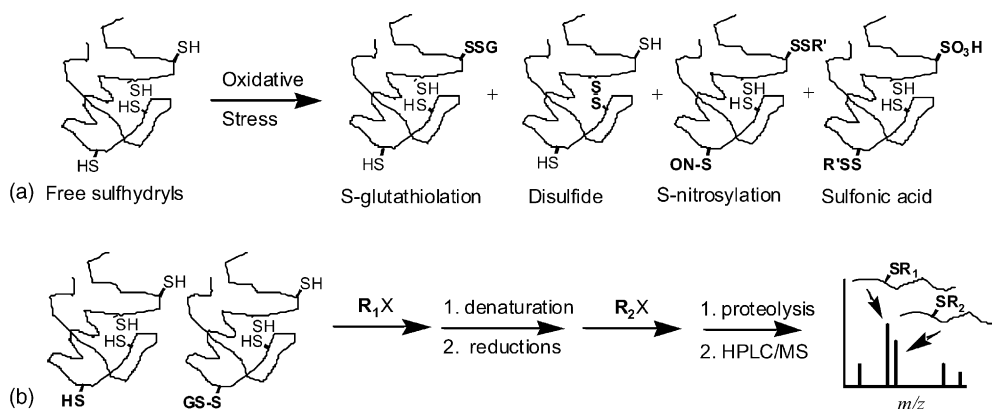
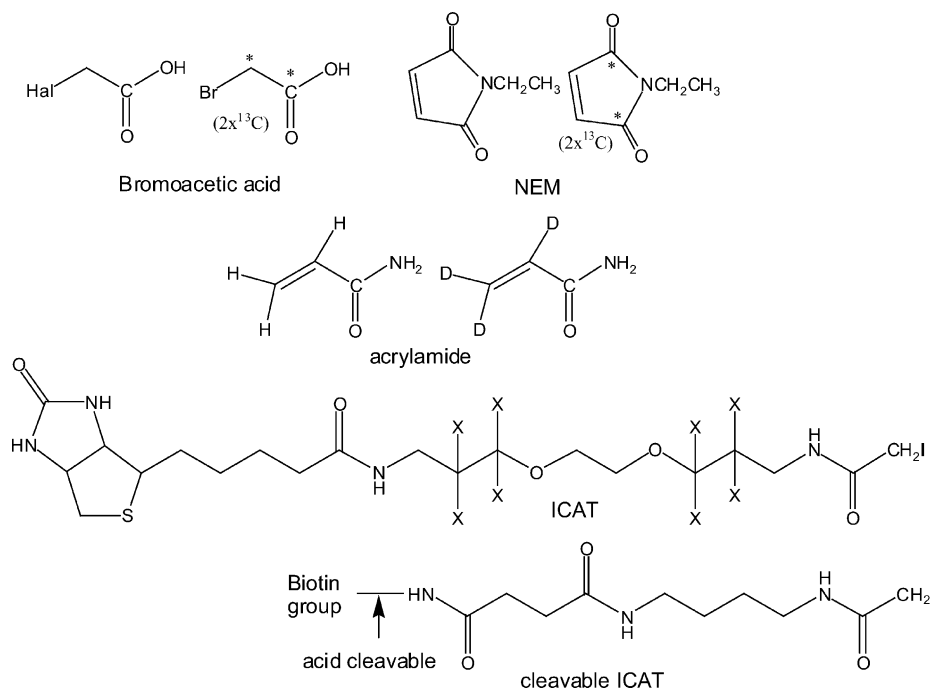


Fig. 2. Differential alkylation strategy using stable isotopes to determine oxidation state of cysteine residues within a protein. Panel A shows a protein containing four free sulfhydryl groups indicating cysteines in their reduced state. Upon oxidative stress these reduced cysteines can get oxidized to form glutathione adducts, intramolecular disulfide bridges (within one protein molecule), intermolecular disulfide bridges (within two protein molecules, dimer formation), and *S*-nitrosylation. These oxidative modifications of cysteine as listed above can be reversed by DTT, whereas under prolonged oxidative stress, cysteine modifications such as oxidation to sulfonic acid are irreversible. Panel B describes differential alkylation where proteins are first alkylated with alkylating reagent 1 (R_1X) to target all freely accessible-sulfhydryl groups (non-oxidized). Then after vigorous denaturation and reduction, proteins are incubated with alkylating reagent 2 (R_2X) an analogous stable isotope reagent to target remaining unreactive (oxidized) cysteines. After proteolysis and HPLC–MS analysis, one can then assign the relative amounts of the reduced versus (reversibly) oxidized cysteine by comparing the ion abundances of the two peptide pairs containing any particular cysteine residue.



Scheme 1. Overview of cysteine alkylating reagents suitable for a differential alkylation strategy indicating the position of stable isotopes with asterisks (*) or X; iodo- and/or bromoacetic acid containing ($2 \times {}^{13}\text{C}$), or ($2 \times {}^{12}\text{C}$); *N*-ethyl-maleimide containing ($2 \times {}^{13}\text{C}$), or ($2 \times {}^{12}\text{C}$); acrylamide in its (d^3) or (d^0) form. Biotin containing reagents are useful for enrichment of cysteine containing peptides and are also available as compounds containing stable isotopes, e.g., isotope coded affinity tag reagents, such as ICAT (d^8/d^0), and acid-cleavable ICAT ($9 \times {}^{13}\text{C}/9 \times {}^{12}\text{C}$).

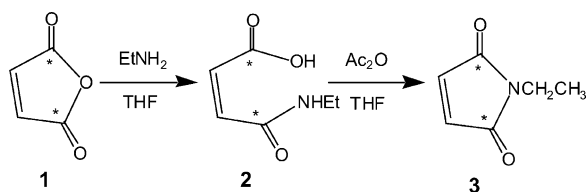
acrylamide reagents: regular acrylamide (d^0), and acrylamide (d^3), and biotin containing, classic isotope coded affinity tag (ICAT) reagents: in their d^0 , and d^8 form; as well as acid-cleavable ICAT reagents: in their $9 \times {}^{12}\text{C}$, and $9 \times {}^{13}\text{C}$ form. In addition to the reagents shown in Scheme 1, other reagents that are currently not available in stable isotope forms may become accessible later, such as 4-dimethylaminophenylazophenyl-4'-maleimide (DABMI), 2,4-dichlorobenzylidoacetamide (IDEnT), or biotin containing reagent PEO-maleimide biotin.

4. Results and discussion

Several mass spectrometric approaches have been described for the assignment of disulfide linkages in proteins and these methods are relevant to the problems of cysteine labeling reactions encountered here. Experimental approaches have been described that involve chemical or proteolytic cleavage of a protein, followed by using mass spectrometry for mass mapping of the disulfide-linked peptides [29,30]. Disulfide linkages can be confirmed by MS/MS or post-source decay (PSD) analysis of the disulfide containing peptide [31,32], or by MS(*n*) analysis of peptides containing intact disulfide bridges [33]. The determination of disulfide linkage often involves several cysteine alkylation steps. For example, Yen et al. [34,35] reported a mass spectrometric method for identification of cysteine disulfide bonds and linkage determination using combina-

tions of chemically different cysteine alkylating reagents and LC/ESI-MS/MS. However, potential systematic problems such as thiol-disulfide exchange and disulfide shuffling can easily occur and have to be considered.

We originally proposed using a differential alkylation strategy to determine the redox state of individual thiols in proteins using stepwise alkylation with common alkylating reagents in combination with stable isotope labeling and mass spectrometric analysis. This novel strategy was first presented at the 51st Annual Meeting of the American Society for Mass Spectrometry [36] (and is now described in full detail in this report). Since this report, Sethuraman et al. [37] published a similar method using an acid-cleavable isotope coded affinity tag and Meza et al. [38] used an analogous strategy (after discussions with Gibson and Schilling) to investigate thiol oxidation in the estrogen receptors. In the work described here, we describe a robust mass spectrometry-based strategy to determine oxidative damage of cysteine residues within proteins. As mentioned above, this protocol is based on differential (stepwise) alkylation of cysteines in combination with stable isotope labeling. Reduced thiols that are readily accessible within the protein are first labeled with common alkylating reagents (RX) containing several stable isotopes (R_1X = i.e. *N*-ethyl-maleimide or iodo/bromoacetic acid), followed by vigorous denaturation and reduction of the protein. The remaining cysteines (initially oxidized, now displayed as free sulfhydryls) are then alkylated with the same alkylating reagent in its normal isotopic form (R_2X). Proteins are then subjected to proteolytic



Scheme 2. Stable isotope containing reagent [1,4- $^{13}\text{C}_2$]-maleic anhydride **1** was reacted with ethylamine in THF at 65 °C for 2 h to form an acid amide intermediate **2**. Subsequent incubation with acetic anhydride in THF at 65 °C for 2 h yielded *N*-ethyl-[1,4- $^{13}\text{C}_2$]-maleimide **3**. Experimental details are described in Section 2.

digestion, and thorough mass spectrometric analysis using MALDI-TOF MS and nano-LC-MS/MS approaches for determination of the cysteine redox state (the ratio of oxidized to reduced state for each individual cysteine residue). The use of NEM reagents within this differential alkylation protocol seems particularly advantageous as maleimides have been described to be highly reactive and to introduce the least chance of disulfide shuffling [35,39].

4.1. Synthesis of isotopically labeled alkylating reagents

To perform the differential alkylating strategy as outlined in Fig. 2, we purchased a set of alkylating reagents, including bromo- and iodoacetic acid labeled with either two, one or no stable isotopes ($2 \times ^{13}\text{C}$, and $1 \times ^{13}\text{C}$, and $2 \times ^{12}\text{C}$) as shown in Scheme 1. For the maleimide reagents we were able to purchase a stable isotope precursor compound, [1,4- $^{13}\text{C}_2$]-maleic anhydride **1** that could then be used to synthesize *N*-ethyl-[1,4- $^{13}\text{C}_2$]-maleimide **3** going through an acid amide intermediate, Compound **2** (see Scheme 2). Ex-

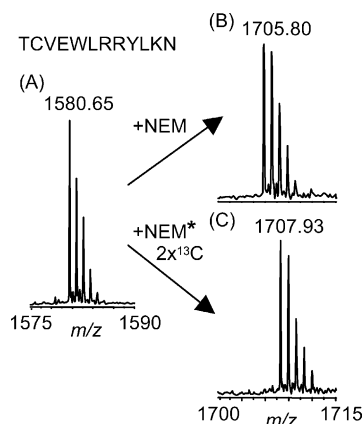


Fig. 3. The MALDI mass spectrum displays molecular ions of standard peptide TCVEWLRRLKKN (major histocompatibility complex antigen H-2K^b fragments 163–174). Panel A shows the non-alkylated peptide with MH^+ at m/z 1580.65 ($M = 1579.64$) that corresponds to a free cysteine sulfhydryl group. Panel B shows peptide TC*VEWLRRLKKN with the Cys residue alkylated with NEM resulting in a shift of the molecular ion MH^+ to m/z 1705.80 ($M = 1704.79$). Panel C shows peptide TC*VEWLRRLKKN with the Cys residue alkylated with stable isotope containing [1,4- $^{13}\text{C}_2$]-NEM resulting in a shift of the molecular ion MH^+ to m/z 1707.93 ($M = 1706.92$).

perimental details are described in Section 2. Both sets of reagents, the halogen-acetic acids and the NEM compounds were then evaluated for the differential alkylation procedure.

4.2. Differential alkylation of standard peptides

The alkylating efficiency of the stable isotope reagents and their mass spectrometric properties was investigated using several commercially available cysteine containing standard peptides. A peptide obtained from the major histocompatibility complex antigen H-2K^b with the sequence TCVEWLRRLKKN was reacted with *N*-ethyl-maleimide in its normal and stable isotope form containing two ^{13}C atoms. Fig. 3 (Panel A) shows the MALDI mass spectrum displaying the

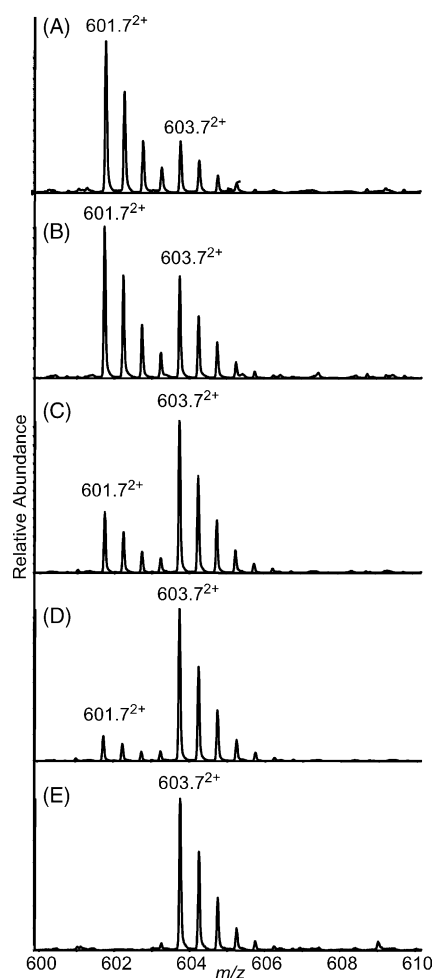


Fig. 4. The ESI-MS spectra show molecular ion isotope patterns of model peptide Arg⁸-Vasopressin (CYFQNCPRG-NH₂), displaying different ratios of alkylating reagent 1 (R_1X : $2 \times ^{12}\text{C}$ -bromoacetic acid) and alkylating reagent 2 (R_2X : $2 \times ^{13}\text{C}$ -bromoacetic acid) that were reacted with the two cysteine residues. Due to the incorporation of stable isotopes (four ^{13}C per peptide), the molecular ion with $[\text{M} + 2\text{H}]^{2+}$ is observed as a doublet ($\Delta M = 4\text{Da}$) at m/z 601.72⁺ ($M = 1201.4$), and at m/z 603.72⁺ ($M = 1205.4$). Isotope patterns correspond to the following ratios of alkylating reagent 1 and alkylating reagent 2. Panel A, $\text{R}_1\text{X}:\text{R}_2\text{X} = 5:1$; Panel B, $\text{R}_1\text{X}:\text{R}_2\text{X} = 2:1$; Panel C, $\text{R}_1\text{X}:\text{R}_2\text{X} = 1:2$; Panel D, $\text{R}_1\text{X}:\text{R}_2\text{X} = 1:5$, and Panel E, $\text{R}_1\text{X}:\text{R}_2\text{X} = 0:1$.

peptide in its native, reduced, non-alkylated form with MH^+ at m/z 1580.65. Upon alkylation with non-isotopically labeled *N*-ethyl-maleimide the peptide generates a molecular ion with MH^+ at m/z 1705.80 (Panel B), whereas the reaction with isotopically labeled *N*-ethyl-[1,4- $^{13}\text{C}_2$]-maleimide yields a peptide with MH^+ at m/z 1707.93 (Panel C). This mass shift of ΔM 2 Da comparing Panels B and C reflects the incorporation of $2 \times ^{13}\text{C}$ atoms per cysteine residue.

A disulfide bridge containing model peptide, Vasopressin (CYFQNCPRG-NH_2), was tested using combinations of bromoacetic acid (R_1X , $2 \times ^{12}\text{C}$), and stable isotope labeled bromo-[1,2- $^{13}\text{C}_2$]-acetic acid (R_2X , $2 \times ^{13}\text{C}$) as alkylating reagents. Fig. 4 shows ESI-MS spectra of the dialkylated peptide featuring different ratios of the reagents displaying the molecular ion $[\text{M} + 2\text{H}]^{2+}$ as a doublet ($\Delta M = 4$ Da) at m/z 601.7 $^{2+}$ ($M = 1201.4$), and at m/z 603.7 $^{2+}$ ($M = 1205.4$). The changes in the isotope pattern clearly correlate with the ratio of incorporated alkylating reagents R_1X and R_2X into the peptide; $\text{R}_1\text{X}/\text{R}_2\text{X}$ was 5:1 (Panel A), 2:1 (Panel B), 1:2 (Panel C), 1:5 (Panel D), and 0:1 (Panel E) simulating different oxidation states of the two cysteine residues. This model peptide ($\text{C}^*\text{YFQNC}^*\text{PRG-NH}_2$) with an alkylating reagent ratio $\text{R}_1\text{X}/\text{R}_2\text{X}$ of 1:2 was then subjected to ESI-MS/MS as shown in Fig. 5. The complete isotope envelope of the molecular ion pair at m/z 601.73 $^{2+}$ and 603.74 $^{2+}$ was selected for CID. An almost complete series of y -ions was observed and several b -ions. The observed fragments that contain one alkylated Cys residue show an isotope pattern of an ion pair with ΔM 2 Da as shown for ion y_4 at m/z 489.2 and 491.2, and for ion y_6 at m/z 731.3 and 733.3 (see insets). The 1:2 ratio within the fragment ion isotope patterns is maintained reflecting the

ratio of $^{12}\text{C}/^{13}\text{C}$ atom incorporation as also observed for the precursor ion at m/z (601.7/603.7) $^{2+}$ (see inset).

4.3. Differential alkylation of proteins and partial oxidation of proteins

To evaluate the differential alkylation strategy to determine oxidative damage or states of cysteine residues within proteins, both PMF and tandem mass spectrometry (nano-HPLC-MS, MS/MS) were employed. Protein subjected to the differential alkylation strategy were digested with trypsin, chymotrypsin, and Glu-C, respectively, and subsequently analyzed by MALDI-TOF mass spectrometry. To extend our protein coverage and to obtain sequence data on individual peptides, the digests were also analyzed by nano-HPLC-MS, MS/MS. The combination of different proteolytic digestion conditions yielded very high combined sequence coverage of the individual proteins.

For aldolase, a protein of 364 amino acid residues with a molecular weight of 39.2 kDa, proteolytic digestions yielded sequence coverages of 65% (trypsin), 69% (chymotrypsin), and 58% (Glu-C), respectively. When combined, an aldolase sequence coverage of 96% was achieved (350 out of 364 residues). In its native state, fructose-bisphosphate aldolase contains 8 Cys residues all in their reduced sulfhydryl form. The different proteolytic digestion conditions allowed us to detect all eight cysteine residues by MALDI-MS in the following proteolytic peptides (listed by their protein residue numbers, and indicating the digestion enzyme): Cys-73 in peptides 63–79 (chym.); Cys-135 in 112–140 (tryp.), 117–138 (chym.), and 134–141 (Glu-C); Cys-150 in 148–153 (tryp.), and 149–162 (chym.); Cys-178 in 174–201 (tryp.), and 175–204 (chym.); Cys-202 in 202–208

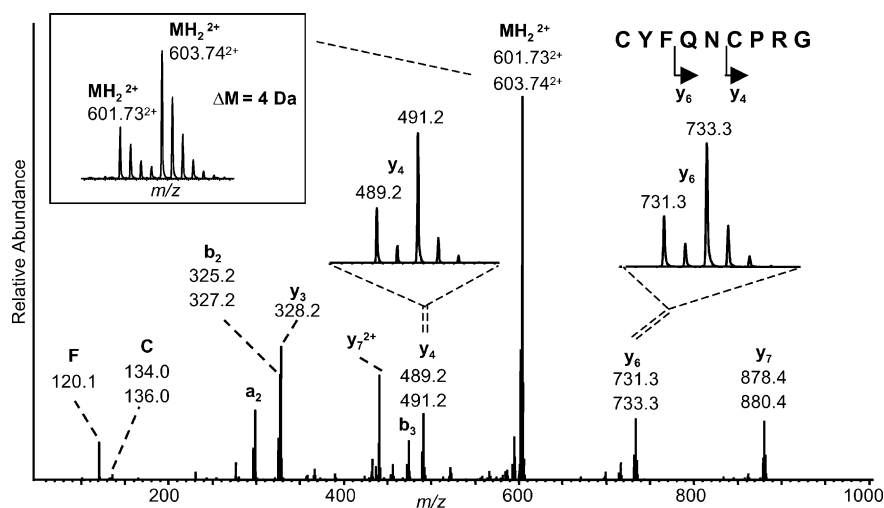


Fig. 5. ESI-MS/MS spectrum of peptide CYFQNCPRG . Cysteine residues are differentially alkylated with alkylating reagent 1, R_1X (bromoacetic acid, yielding $\text{Cys}(\text{R}_1)$) and its stable isotope alkylating reagent 2, R_2X ($[2 \times ^{13}\text{C}_2]$ -bromoacetic acid, yielding $\text{Cys}(\text{R}_2)$). Differential cysteine modification showed a 1:2 ratio of $\text{Cys}(\text{R}_1)$ to $\text{Cys}(\text{R}_2)$ as determined from the molecular ion pattern. The molecular ion consists of an isotope cluster with $[\text{M} + 2\text{H}]^{2+}$ at m/z 601.7 $^{2+}$ ($M = 1201.4$) and at m/z 603.7 $^{2+}$ ($M = 1205.4$) with $\Delta M = 4$ Da (see inset), and was selected for collision induced dissociation (CID). Fragment ions y_4 and y_6 that each contain one modified Cys residue display an isotope pattern with $\Delta M = 2$ Da (see inset) that corresponds to a 1:2 ratio of $\text{Cys}(\text{R}_1)$ to $\text{Cys}(\text{R}_2)$ as expected.

(tryp.), and 175–204 (chym.); Cys-240 in 226–248 (Glu-C); Cys-290 in 285–296 (chym.); Cys-339 in 332–342 (tr.), 329–343 (chym.), and 328–355 (Glu-C). Knowing that we can detect peptides for all eight cysteine residue in the protein, we then applied the differential alkylation strategy, using [1,2- $^{13}\text{C}_2$]-bromoacetic acid as alkylating reagent 1 (R_1X , $2 \times ^{13}\text{C}$) and normal iodoacetic acid as alkylating reagent 2 (R_2X , $2 \times ^{12}\text{C}$), followed by proteolytic digestions. In all cases the cysteine residues reacted with R_1X (>95% [$2 \times ^{13}\text{C}$] stable isotope incorporation) as expected for fully reduced cysteines. The peptides covering all eight cysteine residues (as mentioned above) were now observed shifted by 2 Da per cysteine residue, corresponding to the reaction with the stable isotope form of the alkylating reagent R_1X (causing an incorporation of [$2 \times ^{13}\text{C}$] atoms per Cys alkylation group). No cysteine containing peptide was observed that reacted with the alkylating reagent R_2X that would have indicated an initially oxidized cysteine residue (e.g., disulfide bridge). The control experiment, changing the order of alkylating reagents using the reagent containing no stable isotope as R_1X , and then the stable isotope form as R_1X , yielded cysteine containing peptides without any ^{13}C incorporation as expected for the sulfhydryl cysteines of native aldolase.

After the initial evaluation of differential alkylation strategy using unoxidized aldolase, this protein was partially oxidized with diamide and the same strategy was re-applied. For this experiment, aldolase was incubated at room temperature with different concentrations of a mild oxidizing reagent (diamide) at 10, 50, and 100 μM for times ranging from 0 to 120 min. The protein was then immediately subjected to the stable isotope differential alkylation strategy using the stable isotope version of the alkylating reagent as R_1X (R_1X : [1,2- $^{13}\text{C}_2$]-bromoacetic acid) and R_2X not containing any stable isotopes (R_2X : iodoacetic acid, $2 \times ^{12}\text{C}$) to determine the degree of cysteine oxidation. Fig. 6 shows MALDI-MS spectra recorded after tryptic digestion of aldolase for peptide YASICQQNGIVPIVEPEILPDGDHDLKR (residues Tyr 174 –Arg 201) containing cysteine residue Cys-178. Based on the earlier experiments of unmodified aldolase, molecular ion pairs are expected with MH^+ at m/z 3179.7 (alkylation with R_1X) and m/z 3177.7 (alkylation with R_2X). Without any oxidative stress as shown in Fig. 6 (Panel A) (0 μM diamide, $t = 0$ min) Cys-178 reacted almost completely with R_1X resulting in a molecular ion at m/z 3179.7. The ratio of $\text{R}_1\text{X}/\text{R}_2\text{X}$ of 9:1 indicated its mostly reduced oxidation state. With an increase in oxidative stress the molecular ion isotope pattern shifts from m/z 3179.7 towards m/z 3177.7; $\text{R}_1\text{X}/\text{R}_2\text{X}$ ratios were observed at 60:40 (Panel B, 10 μM diamide, $t = 120$), 30:70 (Panel C, 50 μM diamide, $t = 120$), and finally 0:100 (Panel D, 100 μM diamide, $t = 120$), the distribution reflecting the presence of a fully oxidized Cys-178. Insets within the mass spectra display theoretical isotope patterns simulating the different $\text{R}_1\text{X}/\text{R}_2\text{X}$ ratios as described above.

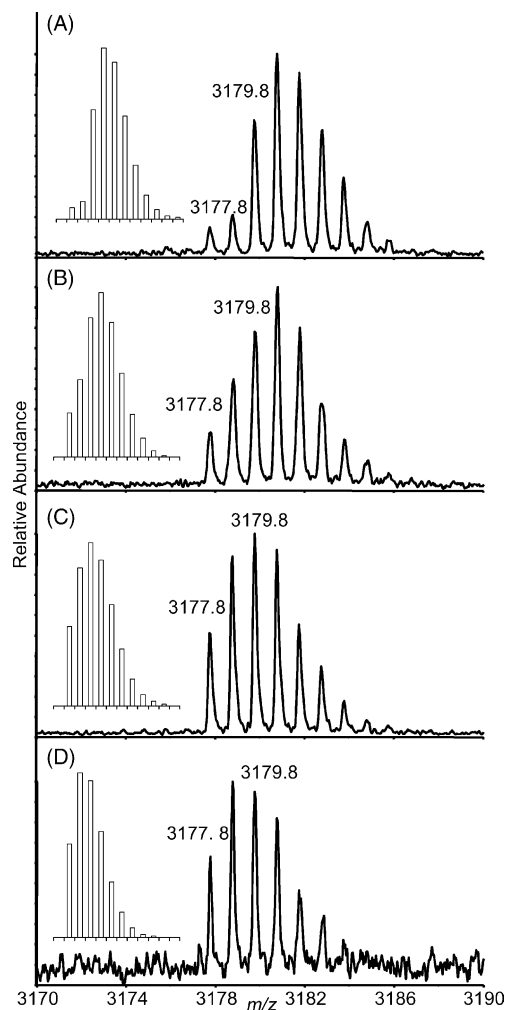


Fig. 6. The MALDI-MS spectra show molecular ion isotope patterns of peptide YASICQQNGIVPIVEPEILPDGDHDLKR (residues Tyr 174 –Arg 201) containing cysteine residue Cys-178 obtained after tryptic digestion of aldolase. Aldolase contains eight cysteine residues that in its native form appear as reduced sulfhydryls. The protein aldolase was incubated with diamide at concentrations of 10, 50, and 100 μM diamide to introduce mild oxidative stress, and subsequently subjected to the differential alkylation protocol (R_1X : $2 \times ^{13}\text{C}$ -bromoacetic acid; R_2X : $2 \times ^{12}\text{C}$ -iodoacetic acid) to determine the degree of cysteine oxidation. Molecular ion pairs with MH^+ at m/z 3179.7 (alkylation with R_1X) and m/z 3177.7 (alkylation with R_2X) were observed as shown in Panels (A) after 0 min diamide incubation (90% $\text{R}_1\text{X}/10\%$ R_2X), (B) after 120 min 10 μM diamide incubation (60% $\text{R}_1\text{X}/40\%$ R_2X), (C) after 120 min 50 μM diamide incubation (30% $\text{R}_1\text{X}/70\%$ R_2X), and (D) after 120 min 100 μM diamide incubation (0% $\text{R}_1\text{X}/100\%$ R_2X). Insets into the MALDI spectra show theoretical isotope patterns for peptide [Y 174 -R 201] simulated according to the $^{12}\text{C}/^{13}\text{C}$ distribution within the cysteine modification (ratio of $\text{R}_1\text{X}/\text{R}_2\text{X}$).

4.4. Irreversible cysteine oxidation to sulfinic and sulfonic acid

The differential alkylation strategy described above was originally designed for determination of reversible cysteine oxidation events, such as Cys disulfide bond formation, Cys-glutathiolation, *S*-nitrosocysteine formation, etc.

Detailed studies that we recently performed on protein characterization of mitochondrial electron transport chain complexes, OXPHOS Complexes I–V (unpublished results) indicated that these multi-protein complexes contain irreversible cysteine oxidation products without any exogenous oxidative treatment. In several cases, we observed Cys-sulfinic (R-SO₂H) and Cys-sulfonic acids (R-SO₃H) in addition to the “regularly” observed cysteine modification, i.e., carbamidomethylation that is formed during reduction and alkylation protocols of cysteines that are present within the proteins in their native reduced or disulfide form. For example, sulfonic acids were observed in OXPHOS complexes, Complex I subunits Ndufs1, and Ndufa5, in Complex II subunits 1–3, and in Complex III subunit 1. In some cases, pairs of peptides containing Cys-sulfonic and Cys-sulfinic acids were observed, such as for Complex II subunit 1 at m/z 874.9²⁺ ($M = 1747.8$, AAFGLSEAGFNTAC^{SO₃H}-ITK), and at m/z 866.9²⁺ ($M = 1731.8$, AAFGLSEAGFNTAC^{SO₂H}-ITK). The identity of the above irreversible Cys modifications was confirmed by nano-LC-ESI-MS/MS. Fig. 7 (Panel A) shows an ESI-MS/MS spectrum of tryptic peptides from Complex III subunit 1 comparing fragmentation of peptide LC*TSATESEVTR (C*: carbamidomethylation). Panel B

shows fragmentation of peptide LC*TSATESEVTR with C* oxidized to a sulfonic acid modification. The precursor ions for regular carbamidomethylated Cys containing peptide was present at an ion count of 706 cps whereas the corresponding sulfonic acid oxidized cysteine containing peptide was observed with a relatively abundant ion count of 236 cps.

5. Conclusions

In the sulfhydryl-labeling strategy described in this report, we used a differential alkylation procedure to label cysteine residues on peptides and proteins as a means to assess their redox status. Some care was given to choosing proper alkylating reagents, such as *N*-ethyl-maleimide, that latter of which is known to have rapid kinetics and to limit the possibility for cysteine disulfide exchange reactions that would complicate any final interpretation as to the precise sites of oxidation. It's our long term plan to now use this strategy to investigate both reversible and irreversible oxidative damage to proteins during disease and aging, especially those targeting cysteine residues. For future studies we aim to apply this differential stable isotope alkylation strategy to identify cysteine oxidation in our Parkinson's disease model, where glutathione depletion *in vivo* leads to a rapid decrease in the activity of Complex I, presumably due to thiol oxidation [25]. As mentioned above, cysteine oxidation is likely to play a major role in Parkinson's disease, particularly affecting the electron transport chain Complex I. As we have now developed several mild one-step protocols to purify Complex I from rodent dopaminergic GSH-depleted cell lines (PD models) and rodent brain (Schilling, Bharath, Andersen, and Gibson, unpublished results), we plan during the next year to examine the over 100 cysteines in Complex I using the method described to investigate the redox status of key cysteine residues as a function of glutathione depletion.

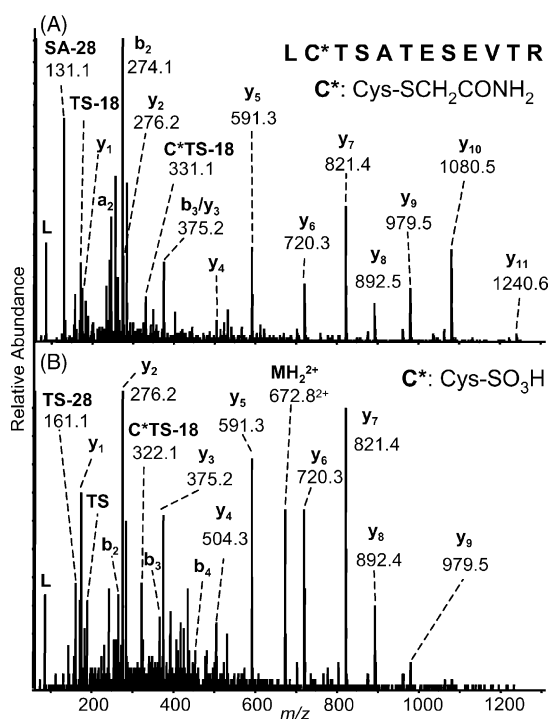


Fig. 7. Tandem mass spectra of tryptic peptides obtained after digestion of electron transport chain multi-protein Complex III (ubiquinol-cytochrome *c* reductase) subunit 1. Panel A shows an ESI-MS/MS spectrum of peptide LC*TSATESEVTR with C* indicating the cysteine as alkylated with iodoacetamide during the digestion protocol yielding a carbamidomethyl modification (precursor ion at m/z 677.3²⁺, $M = 1352.6$). Panel B shows an ESI-MS/MS spectrum of peptide LC*TSATESEVTR with C* indicating the cysteine residue as oxidized to form an irreversible sulfonic acid modification, R-SO₃H (precursor ion at m/z 672.8²⁺, $M = 1343.6$).

Acknowledgements

This work was supported by National Institute of Health grant No. R21 NS43620 (to BWG). BS would like to thank Dr. Gabriel del Rio and Michael Cusack for script writing supporting data analysis.

References

- [1] E.R. Stadtman, Ann. NY Acad. Sci. 928 (2001) 22.
- [2] B.W. Gibson, Sci. Aging Knowledge Environ. 17 (2004) pe12.
- [3] I. Dalle-Donne, D. Giustarini, R. Colombo, R. Rossi, A. Milzani, Trends Mol. Med. 9 (2003) 169.
- [4] J.R. Requena, C.C. Chao, R.L. Levine, E.R. Stadtman, Proc. Natl. Acad. Sci. U.S.A. 98 (2001) 69.
- [5] A. Watanabe, K. Takio, Y. Ihara, J. Biol. Chem. 274 (1999) 7368.
- [6] H. Lindner, W. Helliger, Exp. Gerontol. 36 (2001) 1551.

- [7] M.F. Beal, *Free Rad. Biol. Med.* 32 (2002) 797.
- [8] B. Drew, C. Leeuwenburgh, *Ann. NY Acad. Sci.* 959 (2002) 66.
- [9] M.W. Duncan, *Amino Acids* 25 (2003) 351.
- [10] R.L. Levine, J. Moskovitz, E.R. Stadtman, *IUBMB Life* 50 (2000) 301.
- [11] E.R. Stadtman, J. Moskovitz, R.L. Levine, *Antioxid. Redox Signal* 5 (2003) 577.
- [12] P. Di Simplicio, F. Franconi, S. Frosali, D. Di Giuseppe, *Amino Acids* 25 (2003) 323.
- [13] N.M. Giles, A.B. Watts, G.I. Giles, F.H. Fry, J.A. Littlechild, C. Jacob, *Chem. Biol.* 10 (2003) 677.
- [14] P. Lane, G. Hao, S.S. Gross, *Sci. STKE* 12 (2001) RE1.
- [15] L.B. Poole, P.A. Karplus, A. Claiborne, *Annu. Rev. Pharmacol. Toxicol.* 44 (2004) 325.
- [16] M. Hamann, T. Zhang, S. Hendrich, J.A. Thomas, *Meth. Enzymol.* 348 (2002) 146.
- [17] Y. Wang, S. Vivekananda, L. Men, Q. Zhang, *J. Am. Soc. Mass Spectrom.* 15 (2004) 697.
- [18] R.J. Burns, M.P. Murphy, *Arch. Biochem. Biophys.* 339 (1997) 33.
- [19] T.K. Lin, G. Hughes, A. Muratovska, F.H. Blaikie, P.S. Brookes, V. Darley-Usmar, R.A. Smith, M.P. Murphy, *J. Biol. Chem.* 277 (2002) 17048.
- [20] R.I. Viner, A.G. Krainev, T.D. Williams, C. Schoneich, D.J. Bigelow, *Biochemistry* 36 (1997) 7706.
- [21] R.I. Viner, T.D. Williams, C. Schoneich, *Biochemistry* 38 (1999) 12408.
- [22] L.J. Takemoto, *Biochem. Biophys. Res. Commun.* 223 (1996) 216.
- [23] Z. Gu, M. Kaul, B. Yan, S.J. Kridel, J. Cui, A. Strongin, J.W. Smith, R.C. Liddington, S.A. Lipton, *Science* 297 (2002) 1186.
- [24] K.K. Chung, B. Thomas, X. Li, O. Pletnikova, J.C. Troncoso, L. Marsh, V.L. Dawson, T.M. Dawson, *Science* 304 (2004) 1328.
- [25] N. Jha, O. Jurma, G. Lalli, Y. Liu, E.H. Pettus, J.T. Greenamyre, R.M. Liu, H.J. Forman, J.K. Andersen, *J. Biol. Chem.* 275 (2000) 26096.
- [26] S.R. Jaffrey, H. Erdjument-Bromage, C.D. Ferris, P. Tempst, S.H. Snyder, *Nat. Cell Biol.* 3 (2001) 193.
- [27] H.I. Field, D. Fenyo, R.C. Beavis, *Proteomics* 2 (2002) 36.
- [28] D.N. Perkins, D.J. Pappin, D.M. Creasy, J.S. Cottrell, *Electrophoresis* 20 (1999) 3551.
- [29] J.J. Gorman, T.P. Wallis, J.J. Pitt, *Mass Spectrom. Rev.* 21 (2002) 183.
- [30] J. Qin, B.T. Chait, *Anal. Chem.* 69 (1997) 4002.
- [31] A.R. Cole, N.E. Hall, H.R. Treutlein, J.S. Eddes, G.E. Reid, R.L. Moritz, R.J. Simpson, *J. Biol. Chem.* 274 (1999) 7207.
- [32] M.D. Jones, S.D. Patterson, H.S. Lu, *Anal. Chem.* 70 (1998) 136.
- [33] H. John, W.G. Forssmann, *Rapid Commun. Mass Spectrom.* 15 (2001) 1222.
- [34] T.Y. Yen, R.K. Joshi, H. Yan, N.O. Seto, M.M. Palcic, B.A. Macher, *J. Mass Spectrom.* 35 (2000) 990.
- [35] T.Y. Yen, H. Yan, B.A. Macher, *J. Mass Spectrom.* 37 (2002) 15.
- [36] B. Schilling, S. Bharath, R.H. Row, J.K. Andersen, B.W. Gibson, *Proceedings of the 51st Annual Meeting of the American Society for Mass Spectrometry*, Montreal, Canada, 2003.
- [37] M. Sethuraman, M.E. McComb, T. Heibeck, C.E. Costello, R.A. Cohen, *Mol. Cell Proteomics* 3 (2004) 273.
- [38] J.E. Meza, G.K. Scott, C.C. Benz, M.A. Baldwin, *Anal. Biochem.* 320 (2003) 21.
- [39] W. Zhang, L.A. Marzilli, J.C. Rouse, M.J. Czupryn, *Anal. Biochem.* 311 (2002) 1.